

# Oscillations in the decay law: A possible quantum mechanical explanation of the anomaly in the experiment at the GSI facility

Francesco Giacosa<sup>(a)</sup> and Giuseppe Pagliara<sup>(b)</sup>

We study the deviations from the usual exponential decay law for quantum mechanical systems. We show that simple and physically motivated deviations from the Breit-Wigner energy distribution of the unstable state are sufficient to generate peculiar deviations from the exponential decay law. Denoting with  $p(t)$  the survival probability, its derivative  $h(t)$  shows typically an oscillating behavior on top of the usual exponential function. We argue that this can be a viable explanation of the observed experimental results at GSI Darmstadt, where the function  $h(t)$  has been experimentally measured for electron capture decays of Hydrogen-like ions. Moreover, if our interpretation is correct, we predict that by measuring  $h(t)$  at times close to the initial one, the number of decays per second rapidly drops to zero.

PACS numbers: 03.65.-w, 03.65.Xp, 23.40.-s

## I. INTRODUCTION

In the experimental work of Ref. [1] non-exponential decays of Hydrogen-like ions  $^{140}\text{Pr}$  and  $^{142}\text{Pm}$  have been observed. Denoting  $N(t)$  as the number of unstable particles at the instant  $t$ , one finds that  $dN/dt$  does *not* follow a simple exponential law of the form  $e^{-\lambda t}$ , but shows superimposed oscillations fitted by the following formula:

$$\frac{dN_{dec}}{dt} = -\frac{dN}{dt} \propto e^{-\lambda t} (1 + a \cos(\omega t + \phi)) , \quad (1)$$

where  $dN_{dec}/dt$  represents the number of decay per time (see Fig. 3-5 of Ref. [1]). These unexpected oscillations on top of the exponential decay are known as the ‘GSI anomaly’. The possible explanations of the observed experimental data by invoking neutrino oscillations, neutrino spin precession and quantum beats seem not to be satisfactory, see Refs. [2-7] and refs. therein.

In the framework of non-relativistic quantum mechanics it is indeed known that the exponential decay law is only an approximation, a very a good one, which however holds at late times after the ‘preparation’ of the unstable system, see Refs. [8-11] and refs. therein. By observing the system soon after its preparation, deviations from the exponential decay law occur, which for instance lead to the so called Quantum Zeno effect [12]. Similar properties have been found also in the framework of a genuinely relativistic quantum field theoretical approach [13]. Such deviations are however very difficult to observe because they usually occur on very short time scales, of the order of  $10^{-15}$  s for electromagnetic atomic decays [14] and even shorter for strong decays [13]. A renewed interest in this topic appeared when recent cold atom experiments allowed to clearly observe for the first time deviations from the exponential decay law of unstable systems (via tunneling of atoms out of a trap) [15]. Also the Quantum Zeno effect has found its experimental evidence [16] and there is now a growing area of research related to the so called Quantum Zeno Dynamics [17].

It is tempting to interpret the deviations from the exponential law measured at GSI as a pure quantum me-

chanical effect which has never been observed in the past due to the technical difficulties in doing these kind of experiments. The GSI setup is indeed unique because of its capability of ‘creating’ the unstable states at  $t = 0$ , H-like ions in their case, and to follow their temporal evolution for the first few tens of seconds by single-particle decay spectroscopy. Notice also that they ‘create’ only a few unstable ions for each run of the experiment and collect some thousand measurements to get a good statistics. On the other hand, in a measurement of the decay probability of the same species by using a ‘chunk’ of unstable ions, the effect should be less evident.

In this work we aim to show that it is possible to understand the oscillations such as the ones measured in the GSI experiment by using only quantum mechanics. In fact, oscillations which are qualitatively very similar to the measured ones are obtained as soon as one goes beyond the simple Breit-Wigner [18] form for the mass distribution of the unstable resonance. Indeed, in a simple and solvable model for the decay developed in Ref. [19], oscillations are found at short times and long times after the preparation of the unstable state and represent the transitions from the initial quadratic behavior of the survival probability and the exponential law and then from the exponential law to the power law. Also in the framework of electromagnetic atomic decays, a similar phenomenon has been described in Ref. [14].

## II. DECAY LAW OF QUANTUM SYSTEMS: A PHENOMENOLOGICAL MODEL

In order to discuss our interpretation of the oscillations seen in the GSI experiment, we need first to briefly review the basic formulae concerning the decay law of an unstable state. The decay survival amplitude  $a(t)$  and the survival probability  $p(t)$  can be written as

$$a(t) = \int_{-\infty}^{\infty} dx d(x) e^{-ixt} , \quad p(t) = |a(t)|^2 . \quad (2)$$

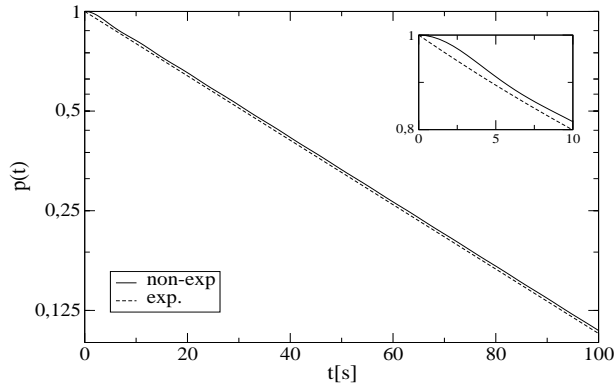


FIG. 1: Survival probability as a function of time for our modified Breit-Wigner distribution (solid line) which shows deviations from the pure exponential decay law (dashed line). The insert displays the deviations from the exponential at times close to  $t = 0$ .

In the Breit-Wigner case one has

$$d(x) \rightarrow d_{BW}(x) = N \frac{\Gamma_0}{(x - M)^2 + \Gamma_0^2/4}, \quad (3)$$

where  $M$  is the mass of the resonance (i.e. its energy in the rest frame),  $\Gamma_0$  its decay width and  $N = 1/2\pi$  is the normalization assuring that  $a(0) = 1$  (the state is prepared at the instant  $t = 0$  with unit probability,  $p(0) = 1$ ). As a consequence, when doing the Fourier transform of the Breit-Wigner distribution, the integral gets only the contribution of the simple pole located at  $x_{pole} = M - i\Gamma_0/2$  leading to

$$a_{BW}(t) = e^{-iMt} e^{-\Gamma_0 t/2}.$$

The usual exponential law for the survival probability, i.e. the probability that the unstable state did *not* decay at the instant  $t$ , emerges:

$$p_{BW}(t) = |a_{BW}(t)|^2 = e^{-\Gamma_0 t}. \quad (4)$$

However, the Breit-Wigner distribution used above is only an approximation, which turned out to be very useful in many practical cases but is nonetheless for very basic reasons not exact, because it relies on the assumption that the spectrum is unbounded from below. Moreover, the average quantities  $\langle E \rangle$  and  $\langle E^2 \rangle$  are not defined. It is therefore expected that far away from the peak the mass distribution  $d(x)$  decreases *faster* than  $1/x^2$ .

In a general framework, the quantity  $\Gamma_0$  should be replaced by a function dependent on the energy,  $\Gamma_0 \rightarrow \Gamma(x)$ . The simple inclusion of an energy threshold,  $\Gamma(x) = 0$  for  $x \leq x_0$ , and provided that the average energy is defined, is already enough to change the properties of the system for both short and large times. In both cases the exponential behavior is not realized: for short times  $p(t)$  shows the quadratic behavior  $p(t) = 1 - \#t^2$ , and for large times a power-law of the kind  $p(t) \sim t^{-n}$

takes place [8]. More in general, when including loops, also the real part of the self-energy –neglected here– would play a role, which assures the correct normalization of the mass distribution (this is a consequence of the Källén-Lehman representation, see Refs. [20, 21] and refs. therein). Concerning the analytical structure of the distribution, as it has been discussed in Ref. [11] within the Lee model, the presence of the branch-cut and the specific details of the form factor determine the deviation from the exponential decay law.

The decay under study in Ref. [1] is a weak decay of an ion with a characteristic decay rate  $\Gamma_0$  of  $1 \text{ min}^{-1}$  and a  $Q$  factor of a few MeV. It is therefore clear that in this case  $\Gamma/M$  is very small and it is technically convenient to perform the change in the integration variable,  $x - M = y$ , thus obtaining:

$$a(t) = e^{-iMt} \int_{-\infty}^{\infty} dy N \frac{\Gamma(y)}{y^2 + \Gamma(y)^2/4} e^{-iyt}. \quad (5)$$

One knows that  $\Gamma(y) \simeq \Gamma_0$  for  $y$  not far from the peak in  $y = 0$ . However, as already remarked before, the distribution far away from the peak should decrease faster than  $1/y^2$ . In this work we take into account this fact by modelling the energy dependence of the decay width  $\Gamma(y)$  in a simple phenomenological way:

$$\Gamma(y) = \Gamma_0 \theta(y + \Lambda_1) \theta(\Lambda_2 - y), \quad (6)$$

where  $\Lambda_1$  and  $\Lambda_2$  are positive numbers, which should be obviously larger than the mean width of the peak  $\Gamma_0$ . We have thus cut the distribution on the left and on the right sides of the peak. These corrections are important because they encode deviations from the Breit-Wigner behavior for values of the energy far away from the peak, whose physical origin lies in the microscopic properties of the form factors and/or in the interaction with the experimental apparatus, see details later on. Independently on the origin of the cutoff(s), the simple parametrization used here is sufficient to show the underlying mechanism and the emergence, as we will discuss in the following, of oscillations superimposed to the exponential decay law in a quite general and understandable framework. In the first section of the Appendix we will also show the results obtained when adopting a function  $\Gamma(y)$  which vanishes smoothly at energies far from the peak.

The survival probability  $p(t)$  represents the probability that a state prepared at  $t = 0$  did not decay at the instant  $t$ . Therefore when  $N_0$  states are present for  $t = 0$ , the number of states changes as  $N(t) = N_0 p(t)$ . In agreement with the experimental analysis of Ref. [1], we are interested in the derivative  $dN/dt$ , i.e. in the number of decays over time  $dN_{dec}/dt$ , which is given by:

$$\frac{dN_{dec}}{dt} = -\frac{dN}{dt} = N_0 h(t) \text{ with } h(t) = -\frac{dp(t)}{dt}. \quad (7)$$

In the previous equation the function  $h(t)$  has been introduced, whose physical interpretation is straightforward:

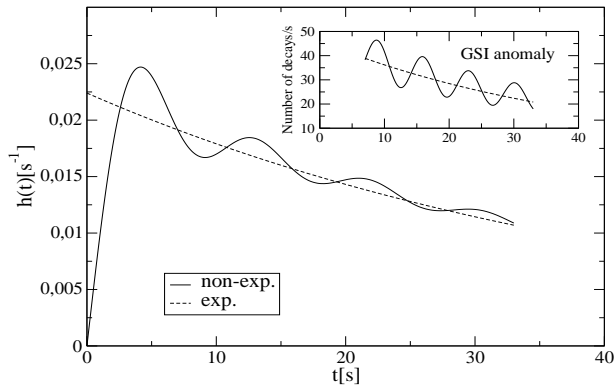


FIG. 2:  $h(t)$  as a function of time for the non-exponential (solid line) and the exponential (dashed line) cases. Sizable oscillations are superimposed on the standard exponential decay for  $t \sim 0$ . The insert shows a fit that was performed in [1] on the data of the GSI anomaly. Our model, having only *one free parameter*, can qualitatively reproduce the observed oscillations. Our curves and the fit have different normalizations.

$h(t)dt$  represents the probability that one unstable state decays within  $t$  and  $t + dt$ . It is also denoted as ‘decay rate’ or ‘decay probability density’.

Let us show now the results we obtain by using our simple model. We focus here on the case of  $^{142}\text{Pm}$  of Ref. [1] for which the total decay rate, obtained from the fit to the data by using the modified exponential, is  $\Gamma_0 = 0.0224 \text{ s}^{-1}$  ( $\sim 10^{-17} \text{ eV}$ ). We use this number as the main time/energy scale in our model. In the present case the threshold  $E_0 \simeq 10^{23}\Gamma_0$  is too far to have any physical effect; moreover, we work with the additional assumption  $\Lambda_1 = \Lambda_2 = \Lambda$ , i.e. the peak is symmetrically restricted on both sides, thus leaving us with only one free parameter. In Fig. 1 we show the survival probability for the numerical choice  $\Lambda = 32\Gamma_0$ : at large times the standard exponential decay law is correctly obtained and at small times (see the insert) sizable deviations from the exponential are present. In Fig. 2 we show the function  $h(t)$  defined in Eq. (7). In the insert we have also displayed the curve obtained in Ref. [1] by fitting the experimental data using Eq. (1). Quite remarkably, we can qualitatively reproduce the oscillations observed in the experiments. A part from the normalization which for us is one but for the experimental fit depends on the number of injected ions, the frequency of the oscillation is correctly reproduced by fixing the only free parameter  $\Lambda = 32\Gamma_0$ .

Two basic differences of our curve w.r.t. the fitting curve of Ref. [1] are visible: (i) the first peak of our oscillations is more pronounced than the others and (ii) the amplitude of the oscillations is, in our case, more suppressed as the time increases. Interestingly, by looking at the data points of Fig. 5 of Ref. [1] both properties (i) and (ii) hold: the first two points are more than  $\sim 2\sigma$  above the exponential curve and the last few points are

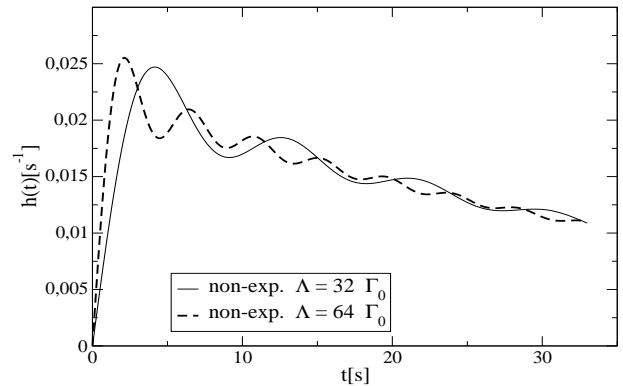


FIG. 3:  $h(t)$  for two different choices of the cutoff. As the cutoff increases, the frequency also increases and the amplitude of the oscillation decreases.

almost on top of the exponential curve. Of course, one would actually need the data to perform a detailed fit within our model and check the value of the  $\chi^2$ , nevertheless, the very fact that the superimposed oscillations naturally emerge is quite exciting and can help to understand the GSI anomaly as a genuine quantum effect.

Moreover, as our Fig. 2 clearly shows, we can make a simple prediction concerning the short time behavior: the function  $dN_{dec}/dt$  is expected to be sizably smaller for  $t \lesssim 5 \text{ s}$  and should tend to zero for  $t \rightarrow 0$ . This is a specific feature of our interpretation of the GSI anomaly and it is related to the well known fact that decay probability approaches  $t = 0$  quadratically as predicted by Quantum Mechanics. If the experiment at GSI could measure a few points below 10 s, our interpretation could be easily rejected or approved.

Let us comment briefly on the dependence of the oscillation frequency  $\omega$  and the amplitude on the specific unstable nucleus. In Ref. [1], there is an indication that  $\omega$  and the amplitude are anti-correlated (only two ions are however examined). This feature is present in our model. In Fig. 3 we show our  $h(t)$  at fixed  $\Gamma_0$  and with cutoffs of  $32\Gamma_0$  and  $64\Gamma_0$ . By increasing the cutoff,  $\omega$  increases and the amplitude (at fixed time) decreases. We will discuss the specific case of the  $^{140}\text{Pr}$  ions in the last section of the Appendix.

### III. INTERPRETATION OF THE GSI ANOMALY

We now comment on the physical interpretation of these oscillations. Similar oscillations of the decay probability have also been found in Ref. [11]. The authors use a nonrelativistic quantum field theory, by employing Lee Hamiltonians, to show that the complicated analytical structure of the propagator in the complex energy plane can be captured by a simple two-pole model: the first pole corresponds to the usual one which defines the

mass and the decay rate of the state, the second pole corresponds instead to the leading order contribution of the branch-cut to the decay amplitude. Interestingly, in their “small coupling limit” they find an exponential decay modulated by oscillation which are qualitatively similar to the ones here presented. A simple physical interpretation emerges: this peculiar behavior of the decay probability interpolates between the pure exponential decay which occurs in presence of a large bandwidth continuum into which the unstable state can decay, and a pure oscillating probability which occurs in a system of two discrete levels where Rabi oscillations are obtained.

In our model, the cutoff regulates the spread of the energy of the continuum of states to which the unstable state is coupled. The oscillating behavior is clearly visible only if the cutoff is smaller than -say-  $100\Gamma_0$ : the unstable state and the continuum are coupled only in a (relatively) small window of energy and thus, as in the two-pole model, the system shows ‘Rabi-like oscillations’ in the decay probability. Besides the similarities, we also point out an important difference w.r.t. Ref. [11]. While in our case the function  $h(t)$  is always positive, the oscillations found in Ref. [11] allow also for zero and negative values of  $h(t)$ ; in that case the Rabi-like oscillations are much stronger.

#### IV. DISCUSSION AND CONCLUSIONS

We now discuss the physical origin of the cutoff that we use to describe the data. A first possibility is that our cutoff emerges as a “natural cutoff” from the calculation of the evolution of the initial unstable state by use of Nuclear Physics models of the nucleus and its weak and electromagnetic interactions with the orbiting electron (e.g. Ref. [22]). For instance, in the case of the electromagnetic atomic decay studied in Ref. [14], such a natural cutoff appears in the wave functions of the electrons and scales as the fine structure constant  $\Lambda \propto \alpha$ . The microscopic calculation of form factors is technically very difficult, we suspect however that it is unlikely that the strong and the electromagnetic interactions, which would be responsible for the form factor for the decay here analyzed, could explain the existence of a cutoff at the energy scale of  $\sim 10^{-16}$  eV needed to describe the GSI result. A second, more promising, possibility is that our cutoff emerges from the interaction of the unstable system and the experimental apparatus. It has been indeed already stressed in Refs. [8, 23, 24] that the measurement itself is an interaction between two physical systems and a cutoff appears which is connected with the finite response time of the experimental apparatus. (Indeed, in Refs. [8, 23] the very same Eq. (6) has been introduced as an effect of the interaction with the measuring apparatus.) During this temporal window the correlation between the unstable state and the decay products is not destroyed by the measurement. The response time is usually very small (and the corresponding cutoff large) for

standard decay experiments. In the GSI experiment, the response time  $\delta t$  should be related, for instance, to the time precision between subsequent observations, which was of the order of one fifth of a second, and/or to the time needed to cool the daughter nucleus before its detection in the storage ring, which was of the order of one second. Remarkably, the inverse of this temporal scale is very close to the cutoff scale  $\Lambda$  used to describe the data ( $\Lambda \sim 1/\delta t$ ). Moreover, in the framework of this interpretation it immediately follows that a repetition of the experiment with an improved time precision (or in general a smaller response time) would correspond to a higher cutoff  $\Lambda$ . For instance, by increasing the time resolution of a factor 2 implies also a cutoff which is larger of a factor 2: as shown in Fig. 3, in this case the amplitude and the period of the oscillations decrease. The very same argumentation can be used to explain why in the experiment at the Berkeley Lab [25] no oscillations have been observed, see also the detailed discussion of this point in Ref. [26]. In the Berkeley experiment the  $^{142}\text{Pm}$  nuclei are embedded in a lattice and are not ionized. When the innermost K-shell electron is captured by the nucleus, an electron from the outer levels jumps to the ground state and a photon is immediately emitted, which is then absorbed by the environment and/or the detector after a very short time delay. In this case, the time-energy uncertainty relation implies that the cutoff is much larger than the decay width,  $\Lambda_{ec} \gg \Gamma_0$ . As visible in Fig. 3, when the cutoff increases the period of the oscillation decreases. Thus, in the case of the Berkeley experiment the oscillations are extremely suppressed and cannot be detected. Our approach, together with the assumption of a cutoff induced by the measurement, can explain in a rather natural way the absence of oscillations in the experimental setup of Ref. [25]. Furthermore, it is also possible to study the other decay channel of  $^{142}\text{Pm}$ , the  $\beta^+$  process, and to explain why also in this case no oscillations should be observed (see section A.2 in the Appendix).

Another subtle issue emerges when trying to interpret the results of the GSI by using the standard “projection postulate” of Quantum Mechanics: in an ideal measurement the collapse of the wave function, and thus the measurement itself, occurs instantaneously as soon as the wave function of the unstable system interacts/overlaps with the measurement apparatus. In this sense the measurement effectively “resets the clock” every time the unstable system is found to be undecayed and what could be measured, at the storage ring of the GSI for instance, is just an exponential decay, which is slowed down (quantum Zeno effect) or accelerated (quantum Anti-Zeno effect) depending on the details of the unstable state and on the time interval of the pulsed measurements. On the other hand, the measurement at the GSI experiment is quite peculiar: the system “sees” (in the frequency spectrum) the ions averagely every  $\sim 200$  ms and not at every passage through the mass spectrometer, which occur every  $0.5\mu\text{s}$ . Moreover, as discussed before, the appearance

in the frequency spectrum of the daughter ions is delayed by 900 and 1400 ms (for  $^{140}\text{Pr}$  and  $^{142}\text{Pm}$  respectively) needed for the cooling. This means that there is a period of about 1 s during which the experimental apparatus does not “see” neither the parent ion nor the daughter ion. This measurement clearly is not an ideal measurement: a detailed modelling of the innovative and unique measuring procedure used at GSI on the line of the theory of measurement described in Refs. [23, 24, 27] deserves further investigation. Notice also that, within our interpretation, the experiment at GSI would be a precious experimental apparatus for the study of the fundamental open questions related to the process of measurement in Quantum Mechanics.

In conclusions, we have studied in a general framework a typical behavior of unstable particles: exponential decay law with superimposed oscillations. We have shown that this behavior is quite common as soon as the Breit-Wigner distribution of the unstable state is left and (even very simple) form-factors are taken into account, which suppress the Breit-Wigner distribution far away from the peak. Using a cut-off model, we have shown that we can reproduce the qualitative behavior of the oscillations seen in the GSI experiment. Obviously, the adopted modification represents a first attempt to investigate how the oscillations in the decay law emerge. Future work in this direction should go beyond the simple cutoff. For instance, the detailed modelling of the measurement should also naturally provide how the energy distribution deviates from the Breit-Wigner form. However, independently on the details of the deviations from the Breit-Wigner form, if our interpretation is correct, we predict that, for times smaller than 5 s (see Fig. 2), the number of decays per seconds rapidly drops to zero due to a fundamental property of quantum systems: the quadratic behavior of the survival probability at short times after the preparation of the system. Moreover, we also predict that the first oscillation is more pronounced than the others.

Finally, we would like to mention that possible indications of the presence of oscillations superimposed to the exponential decay were found also in two other unstable, but utterly different, quantum systems: the tunneling of cold atoms out of a trap [15] and the decay of  $^{32}\text{Si}$  [28]. In particular, in the latter case, the unstable nuclei  $^{32}\text{Si}$  have a very large half-life of about 170 yr, but show superimposed oscillations of about 1 yr. We speculate that also these superimposed oscillations represent a manifestation of the same fundamental phenomenon of Quantum Mechanics.

**Acknowledgments:** The authors thank G. Torrieri and H. Warringa for pointing out Refs. [1,19] and A. Merle for very useful comments. G.P. acknowledges financial support from the Italian Ministry of Research through the program “Rita Levi Montalcini”.

## Appendix A

In this appendix we discuss in more details three subjects: the existence of oscillations for smooth form factors, the inclusion of two decay channels and finally the case of the decay of the  $H$ -like  $^{140}\text{Pr}$  ions also measured at GSI.

### 1. Oscillations upon variation of form factors

The existence of oscillations does not depend on the precise form of the cutoff. In Ref. [26] the cases in which only one end is open have been tested. Here we study the oscillations by introducing a Fermi-like cutoff function of the form:

$$a(t) = N \int_{-\infty}^{\infty} \frac{\Gamma(y)}{y^2 + \Gamma^2(y)/4} \quad (\text{A1})$$

$$\Gamma(y) = \frac{\Gamma_0}{1 + e^{-\alpha^2(y^2 - \Lambda^2)}}, \quad (\text{A2})$$

where the constant  $\alpha$  controls the steepness of the fall-off for  $y \simeq \pm\Lambda$ . In Fig. 4, we show the results obtained for  $h(t)$  for three different choices of the parameter  $\alpha$ . Clearly the smaller the value of  $\alpha$  the smaller are the oscillations superimposed to the exponential decay. This fact has a natural explanation by reminding that the oscillations are present only if the bandwidth of the continuum of states into which the unstable state decays is narrow, as explained before. We notice on the other hand that it is possible to obtain very large oscillations (with  $h(t)$  reaching even negative values) within the two pole model proposed in [11]. More in general, one can extend the present study by investigating more complicated forms of the function  $\Gamma(y)$ . This represents an interesting outlook for future work.

### 2. Two channels

We turn now to the non-exponential decay when two decay channels are present. To this end we use the formalism developed in Ref. [29]. The total energy-dependent decay width reads  $\Gamma(y) = \Gamma_1(y) + \Gamma_2(y)$ , where  $\Gamma_i(y)$  represent the energy-dependent decay width in the  $i$ -th channel. The survival probability amplitude  $a(t)$  can be decomposed as the sum of two terms:

$$a(t) = N \int_{-\infty}^{\infty} \frac{\Gamma(y)}{y^2 + \Gamma^2(y)/4} = a_1(t) + a_2(t) \quad (\text{A3})$$

whereas  $N$  assures that  $a(0) = 1$  and

$$a_1(t) = N \int_{-\infty}^{\infty} \frac{\Gamma_1(y)}{y^2 + \Gamma^2(y)/4}, \quad (\text{A4})$$

$$a_2(t) = N \int_{-\infty}^{\infty} \frac{\Gamma_2(y)}{y^2 + \Gamma^2(y)/4}. \quad (\text{A5})$$

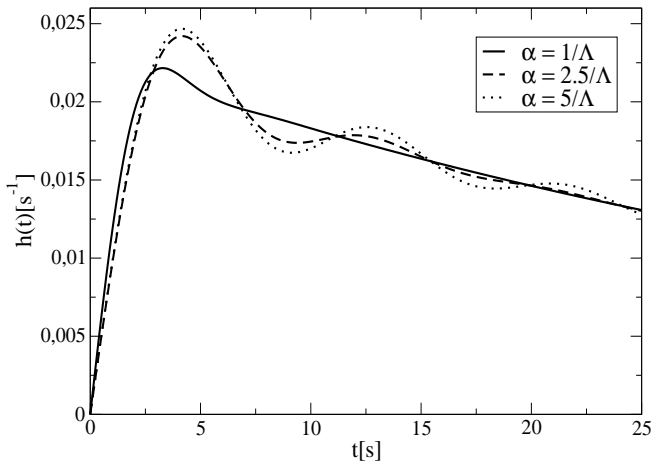


FIG. 4:  $h(t)$  is shown in the case of a smooth cutoff function (Fermi-like). The smaller the value of  $\alpha$  the smaller the oscillations are.

The decay probability densities per each channel  $h_1(t)$  and  $h_2(t)$  read [29]:

$$h_1(t) = -A'_1(t) - A'_{mix}(t), \quad h_2(t) = -A'_2(t) - A'_{mix}(t) \quad (\text{A6})$$

with

$$A_1(t) = |a_1(t)|^2, \quad A_2(t) = |a_2(t)|^2, \quad (\text{A7})$$

$$A_{mix}(t) = \text{Re} [a_1(t)a_2^*(t)]. \quad (\text{A8})$$

In the case of the  $H$ -like ion  $^{142}\text{Pm}$ , one has that  $\Gamma_{ec} = \Gamma_1(y=0) = 0.2\Gamma_0$  corresponds to the electron-capture decay  $M \rightarrow D + \nu_E$ , and that  $\Gamma_{\beta^+} = \Gamma_2(y=0) = 0.8\Gamma_0$  corresponds to the  $\beta^+$  decay  $M \rightarrow D' + e^+ + \nu_E$ . Moreover, following the discussion in the text, we assign a different cutoff per each channel:  $\Gamma_1(y) = \Gamma_{ec}\theta(y^2 - \Lambda_{ec}^2)$  and  $\Gamma_2(y) = \Gamma_{\beta^+}\theta(y^2 - \Lambda_{\beta^+}^2)$ .

As described in Sec. II, for the ion  $^{142}\text{Pm}$  a cutoff  $\Lambda_{ec} = 32\Gamma_0$  reproduces the correct oscillation frequency. The origin of  $\Lambda_{ec}$  can be traced back either to a (quite unnatural) microscopic form factor or to (more plausible) measurement apparatus effect via the time-energy uncertainty relation,  $\Lambda_{ec} \sim \frac{1}{\delta t} \sim 10^{-15}$  eV. In the latter case, we can easily estimate the cutoff  $\Lambda_{\beta^+}$  in the  $\beta^+$ -channel. The positron is emitted with an energy within 0-4 MeV. For our estimate let us consider a positron with 2 MeV, which corresponds to a speed of  $v_{e^+} \simeq 0.96c$ . Thus, the positron is absorbed very fast by the environment. Assuming that it travels 1 m, we get  $\delta t \simeq 10^{-9}$  s. In turn, the cutoff in this channel reads  $\Lambda_{\beta^+} \sim 10^{-7}$  eV, which corresponds to roughly  $10^9\Gamma_0$ .

In Fig. 5-6 we show the functions  $h_1(t)$  and  $h_2(t)$ . The function  $h_1(t)$ , which describes the decay probability density in the electron-capture decay channel, shows a behavior which is very similar to the one of Fig. 3 in which the  $\beta^+$  decay channel was not considered. On the contrary, the function  $h_2(t)$ , which describes the decay

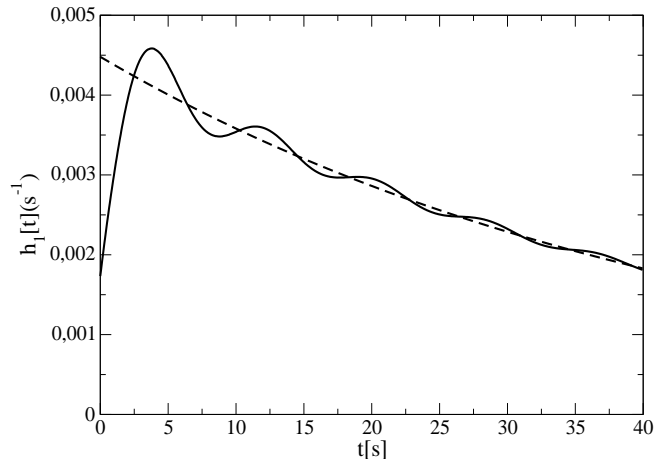


FIG. 5: Decay rate  $h_1$  for the electron capture channel. The dashed line corresponds to the exponential decay.

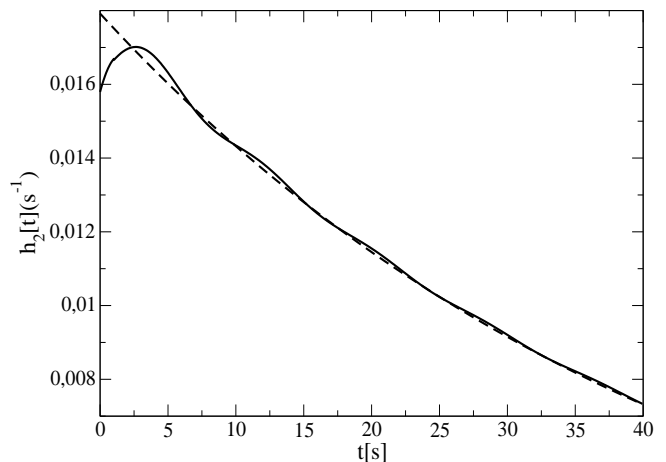


FIG. 6: Decay rate  $h_2$  for the  $\beta^+$  channel. The dashed line corresponds to the exponential decay.

probability density in the  $\beta^+$  decay channel, is not distinguishable from an exponential decay for times larger than  $\sim 5$ s. Notice that, for our choice of parameters, the first peak is present also in the  $\beta^+$  channel due to the mixing of the two channels implied by formulae (A6). On the other hand, by fixing also  $\Lambda_{ec}$  to be large (as in the case of the Berkeley experiment), both  $h_1$  and  $h_2$  would be basically pure exponential laws.

### 3. Changing the $H$ -like ion

As a last step, we briefly comment on the decay of the other ion,  $^{140}\text{Pr}$ , measured in Ref. [1]. The modulation frequency for  $^{140}\text{Pr}$  is slightly higher than the

one of  $^{142}\text{Pm}$  ( $0.890\text{ s}^{-1}$  and  $0.885\text{ s}^{-1}$  respectively). In our interpretation, if the cutoff originates from the experimental apparatus and in particular from its response time (temporal resolution and cooling time as discussed before), we expect a mild dependence from the mass number  $A$  and charge  $Z$  of the nucleus. The cooling times for the decay products of  $^{140}\text{Pr}$  and  $^{142}\text{Pm}$  are respectively 900 ms and 1400 ms (corresponding to their different recoil energy). By assuming that the temporal resolution for the two ions is the same, one would expect that

the modulation frequency of  $^{140}\text{Pr}$  is larger than the one of  $^{142}\text{Pm}$  as the data seem to indicate. Again, at this level, it is complicated to provide quantitative estimates and moreover it would be mandatory to experimentally check the dependence of the modulation frequency from the nucleus by using other species and with more accurate precision.

- 
- [1] Y. Litvinov, F. Bosch, N. Winckler, D. Boutin, H. Essel, et al., *Phys. Lett.* **B664**, 162 (2008).
- [2] A. G. Cohen, S. L. Glashow, and Z. Ligeti, *Phys. Lett.* **B678**, 191 (2009).
- [3] A. Gal, *Nucl. Phys. A* **842** 102 (2010).
- [4] A. Merle, *Prog. Part. Nucl. Phys.* **64**, 445 (2010).
- [5] A. Merle, *Phys. Rev.* **C80**, 054616 (2009).
- [6] J. Wu, J. A. Hutasoit, D. Boyanovsky, and R. Holman, *Phys. Rev.* **D82**, 045027 (2010).
- [7] C. Giunti, arXiv:0801.4639 [hep-ph]. A. N. Ivanov, E. L. Kryshen, M. Pitschmann and P. Kienle, arXiv:0807.2750 [nucl-th]. C. Giunti, arXiv:0807.3818 [hep-ph]. H. Burkhardt, J. Lowe, G. J. Stephenson, Jr., T. Goldman and B. H. J. McKellar, arXiv:0804.1099 [hep-ph]. M. Peshkin, arXiv:0804.4891 [hep-ph].
- [8] L. Fonda, G. C. Ghirardi, and A. Rimini, *Reports on Progress in Physics* **41**, 587 (1978).
- [9] A. Peres, *Annals Phys.* **129** (1980) 33; G. Garcia-Calderon, V. Riquer, and R. Romo, *J. Phys. A Math. Gen.* **34**, 4155-4165 (2001).
- [10] H. Nakazato, M. Namiki, and S. Pascazio, *Int. J. Mod. Phys. B* **10**, 247 (1996).
- [11] P. Facchi and S. Pascazio, *Quantum Probability and White Noise Analysis* **17**, 222 (2002).
- [12] B. Misra and E. C. G. Sudarshan, *Journal of Mathematical Physics* **18**, 756 (1977).
- [13] F. Giacosa and G. Pagliara, *Mod. Phys. Lett. A* **26**, 2247 (2011); G. Pagliara and F. Giacosa, *Acta Phys. Polon. Supp.* **4** 753 (2011).
- [14] P. Facchi and S. Pascazio, *Phys. Lett. A* **241**, 139 (1998).
- [15] S. R. Wilkinson, C. F. Bharucha, M. C. Fischer, K. W. Madison, P. R. Morrow, Q. Niu, B. Sundaram, and M. G. Raizen, *Nature* **387**, 575 (1997).
- [16] M. C. Fischer, B. Gutiérrez-Medina, and M. G. Raizen, *Phys. Rev. Lett.* **87**, 040402 (2001).
- [17] P. Facchi and S. Pascazio, *Journal of Physics A* **41**, 3001 (2008).
- [18] G. Breit, *Handbuch der Physik* **41**, 1 (1959).
- [19] R. G. Winter, *Phys. Rev.* **123** 1503 (1961). See also further developments in: D. A. Dicus, W. W. Repko, R. F. Schwitters, and T. M. Tinsley, *Phys. Rev. A* **65**, 032116 (2002) and in J. Levitan, *Phys. Rev. A* **129**, numbers 5,6.
- [20] N. N. Achasov and A. V. Kiselev, *Phys. Rev.* **D70**, 111901 (2004).
- [21] F. Giacosa and G. Pagliara, *Phys. Rev.* **C76**, 065204 (2007).
- [22] W. Bambynek, H. Behrens, M. Chen, B. Crasemann, M. Fitzpatrick, et al., *Rev. Mod. Phys.* **49**, 77 (1977).
- [23] A. Degasperis, L. Fonda and G. C. Ghirardi, *Nuov. Cim.* **21** 471 (1974).
- [24] K. Koshino, A. Shimizu, *Phys. Rep.* **412**, 191 (2005).
- [25] P. A. Vetter, R. M. Clark, J. Dvorak, K. E. Gregorich, H. B. Jeppesen, S. J. Freedman, D. Mittelberger and M. Wiedeking, *Phys. Lett. B* **670** (2008) 196 [arXiv:0807.0649 [nucl-ex]].
- [26] F. Giacosa and G. Pagliara, proceedings contribution to the "50th International Winter Meeting on Nuclear Physics", 23-27 January 2012, Bormio, Italy, arXiv:1204.1896 [nucl-th].
- [27] A. G. Kofman, G. Kurizki, *Phys. Rev. Lett.* **87**, 270405-1 (2001).
- [28] D. E. Alburger, G. Harbottle, and E. F. Norton, *Earth and Planetary Science Letters* **78**, 168 (1986).
- [29] F. Giacosa, arXiv:1110.5923 [nucl-th].